Appl. Phys. B 87, 603–606 (2007)
DOI: 10.1007/s00340-007-2676-9

Applied Physics B
Lasers and Optics

Y. SHENG✉
J. DOU
B. CHENG
D. ZHANG

Effective generation of red-green-blue laser in a two-dimensional decagonal photonic superlattice

Optical Physics Lab., Beijing National Laboratory for Condensed Matter Physics, Institute of Physics, Chinese Academy of Sciences, Beijing 100080, P.R. China

Received: 12 February 2007 / Revised version: 24 April 2007
Published online: 24 May 2007 • © Springer-Verlag 2007

ABSTRACT We demonstrate the effective generation of red, green and blue (RGB) light in a two-dimensional decagonal quasiperiodic $LiNbO_3$ nonlinear crystal. Owing to the unique abundance in reciprocal vectors (RVs), the RGB signals were generated directly by frequency doublings. Thus the conversion efficiencies of the RGB light were much higher than previously recorded. In addition, the same results were obtained when the crystal was rotated by integral multiples of $\pi/5$. This result will aid in the effective generation of RGB in multiple directions and may have important applications in laser-based projection displays.

PACS 42.65.Ky; 42.72.Bj; 42.79.Nv

1 Introduction

The three colors of the red, green and blue laser source are needed more frequently since most visual colors including white light can be produced by combining these three primary colors in the proper proportion. Optical frequency conversion with nonlinear optical materials is an important means for achieving such sources. Thus considerable attention has been given to this field. For example, observations of quasiphase matching of RGB using a proton exchanged $LiNbO_3$ waveguide [1] and using a dye-doped polymer waveguide [2] were reported. For bulk samples, results were mainly obtained via sum-frequency mixing, frequency doubling or optical parametric oscillation following a cascaded second-order process [3–10].

However, the cascaded harmonic or sum-frequency generation may be not a good candidate. It usually fails to yield a vigorous output due to its inherently low efficiency. As for optical parametric oscillation, additional dielectric coatings on the sample's head faces are needed to form an optical oscillator cavity. In addition, it must run at high temperatures to prevent photorefractive damage. Attempts at the generation of RGB by frequency doublings using a one-dimensional aperiodic optical superlattice have been made [11, 12], but the efficiency experimentally attained was still comparatively low [13]. The involved enormous computer procedures and inevitable deviations between theoretical design and experiment add to the complexity in using them as practical devices. Thus the effective generation of the three primary colors is still a challenge.

In this work, we substituted a two-dimensional decagonal quasiperiodic superlattice for the traditional one-dimensional structure. On the basis of which, plentiful reciprocal vectors were achieved to produce RGB signals directly by frequency doublings. Therefore, the output efficiency of RGB light obtained is much higher than previously documented, and no special treatment is needed. Even though a decagonal quasicrystal was recently reported as a means to broaden the harmonic temperature and wavelength acceptance bandwidth [14], no record of it as a RGB light generator was found.

✉ Fax: +86-10-82649531, E-mail: shengyan@aphy.iphy.ac.cn

2 Experiments

2.1 *Structure and diffraction pattern of decagonal quasiperiodic superlattice*

The two-dimensional decagonal quasiperiodic superlattice was fabricated by the electric field poling technique in a z-cut $LiNbO_3$ wafer [15]. Figure 1 shows the microscopic $+z$ surface of the etched sample, in which the quasiperiodic geometric tiling with tenfold symmetric axis is displayed. It was composed of thin rhombi (with vertex angles of 36° and 144°) and thick rhombi (72° and 108°). The side length of the rhombi was about $a = 13.19\,\mu m$. The poled circular cylinders placed at the vertices of rhombi and their diameter was about 5.2 μm. No domain merging was found across the whole sample of $9.5 \times 9.5 \times 0.4\,mm^3$.

Figure 2a is the diffraction pattern of the crystal with its local tenfold axis parallel to the incident He-Ne laser. The pattern possesses tenfold rotational symmetry, with four series of the most intense peaks visible. The magnitude and orientation of the RVs of the internal series correspond to the inverse of half the long diagonal of the thin rhombi. Similarly, the external three series, respectively, correspond to half the long diagonal of the thick rhombi, half the side length, and half the short diagonal of the thin rhombi. We choose the RVs for the internal series of spots to form

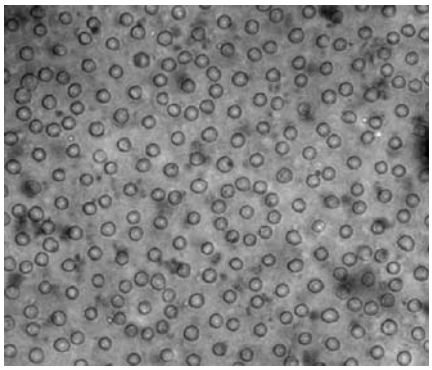

FIGURE 1 The $+z$ face micrograhps of poled $LiNbO_3$ crystal in a decagonal quasiperiodic manner

a basic set $\pm \boldsymbol{F}_i$ $(i = 1, ..., 5)$, where

$$\boldsymbol{F}_1 = (1, 0) = (10000)$$
$$\boldsymbol{F}_2 = (\cos(\pi/5), \sin(\pi/5)) = (01000)$$
$$\boldsymbol{F}_3 = (\cos(2\pi/5), \sin(2\pi/5)) = (00100)$$
$$\boldsymbol{F}_4 = (\cos(3\pi/5), \sin(3\pi/5)) = (00010)$$
$$\boldsymbol{F}_5 = (\cos(4\pi/5), \sin(4\pi/5)) = (00001)\,.$$

In the above equations, the vectors are expressed in both two-dimensional Cartesian coordinates and in a symbolic five-dimensional vector notation. The magnitude of each $\boldsymbol{F}_i$ is related to the side length as $|\boldsymbol{F}_i| = 2\pi/(a\cos(\pi/10)) \approx 1.051 \times 2\pi/a$ [16, 17]. Figure 2b is the schematic view of part spots in the reciprocal vectors, in which the real-line arrows $\boldsymbol{F}_i$ $(i = 1, 2, 3, 4, 5)$ indicate five basic reciprocal vectors. When we choose the basic set of RVs, it is possible to index the entire diffraction pattern. The intensities of the diffraction peaks related to the different prominent series, their indexes and the related elements of the tiles defining the quasicrystal, are shown in Table 1.

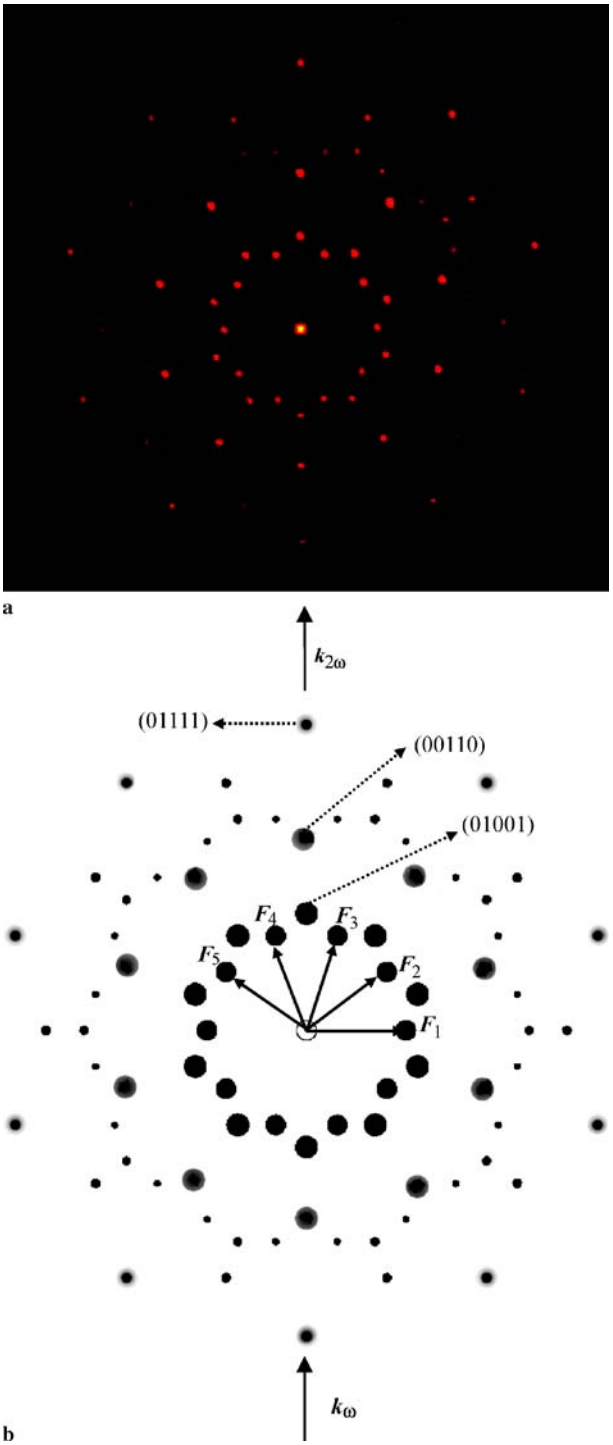

FIGURE 2 (**a**) The diffraction patterns of $LiNbO_3$ nonlinear crystal with its local tenfold axis parallel to the He-Ne beam. (**b**) Schematic view of the reciprocal vectors. The real-line arrows $\boldsymbol{F}_i$ $(i = 1, 2, 3, 4, 5)$ indicate the five basic reciprocal vectors. The direction of input and output beams is along reciprocal vector (01011) in the collinear QPM harmonic generations

2.2 *Experiments of red, green and blue light generation by frequency doubling*

The quasiphase matching condition in the frequency doubling process can be written as $\Delta k = k_{2\omega} - 2k_\omega - G_{m,n,o,p,q}$, where Δk is the wave vector mismatching, k_ω and $k_{2\omega}$ are the wave vectors of fundamental and harmonic waves, and $G_{m,n,o,p,q}$ is the reciprocal vector which depends on the combination of the five basic RVs. Different from the periodic RVs that can be simply indexed with one or two integers, the indexing of the five basic RVs requires five integers in a decagonal system.

The performance of the decagonal quasicrystal as a generator of red, green and blue light was experimentally detected at room temperature. The fundamental source was a tunable nanosecond optical parametric oscillator pumped by a Nd:YAG laser. Its repetition rate and pulse width were 10 Hz and 4 ns, respectively. The incident fundamental beam was s-polarized and entering along the

RV	Magnitude	Fourier coefficient	Associated element of the tile
(10000)	1.000	1.000	Half long diagonal of thin rhombi
(01001)	1.176	1.201	Half long diagonal of thick rhombi
(00110)	1.902	0.922	Half side length
(01111)	3.078	0.343	Half short diagonal of thin rhombi

TABLE 1 Magnitudes and intensities of different Fourier coefficients of the decagonal quasiperiodic structure

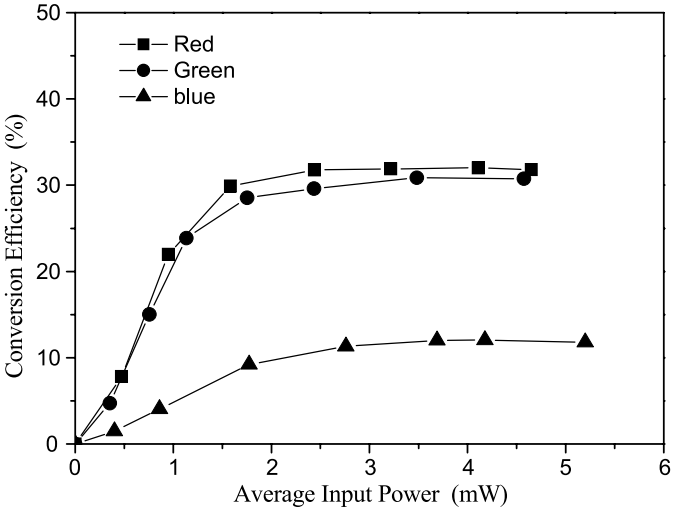

FIGURE 3 Conversion efficiencies of RGB light generation as a function of average input power

RV (01001). It was weakly focused by a 15 cm focal-lens that produced a focal spot with a diameter of 180 μm. When the fundamental beam was at 1.249 μm, 1.061 μm and 0.915 μm, respectively, the three primary colors were generated as their frequency doublings. In these processes the reciprocal vectors (01001), (00110) and (01111) were individually responsible for the phase matching. The length of RV (00110) is longer than that of (01001) by a factor of $(1+\sqrt{5})/2$, and (01111) is equal to the sum of (00110) and (01001).

In Fig. 3, the average output power as a function of average input power is shown, in which squares, dots and triangles represent the experimental values of red light at 624.5 nm, green at 530.5 nm and blue at 457.5 nm, respectively. The higher conversion efficiencies of 31.8% for the red, 29.6% for green and 11.3% for blue were generated when the average input powers were 2.44, 2.43 and 2.76 mW, respectively. In principle, the second harmonic conversion efficiency increases proportionally with the input power and occurs when using a moderate input. However, in our case the input powers were quite high, so that the harmonic outputs could be affected by a number of factors. The major factor can be attributed to back conversion, as pointed out by Hanna [18]. Meanwhile, the divergence of input light (a slightly focused beam was used in our experiment) and the small irregular distribution of the reversed domains (as shown in Fig. 1) could directly impact the phase matching condition. All of these result in a saturation effect of the second harmonic output at a higher input power. Such an effect has been observed in experiments of periodic structures [18, 19]. Even though the obtained conversion efficiency of blue light was about one order of magnitude higher than previously recorded, it is still weaker compared with that of red and green. This may result from the following two factors: the Fourier coefficient of the adopted reciprocal vectors and the poled column diameter of the crystal, which are similar to the phenomena in the two-dimensional periodic poled $LiNbO_3$ [15].

We measured the wavelength acceptance bandwidths around 1.249, 1.061 and 0.915 μm with an average power of 2.0 mW. The results are shown in Fig. 4. The FWHM of the experimental curve is 2.0 nm, 1.3 nm and 0.8 nm, respectively.

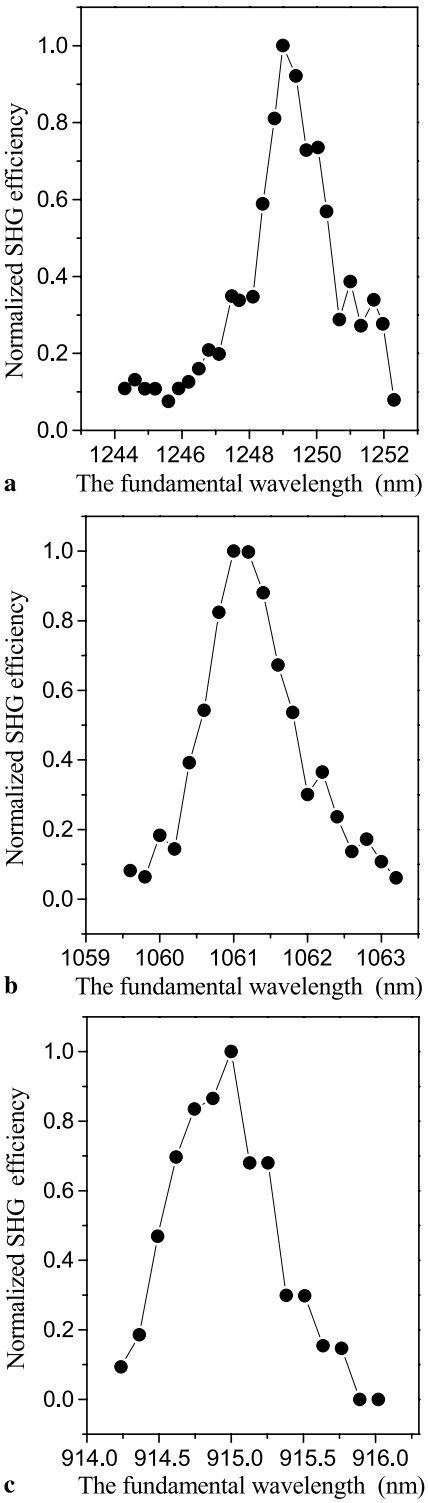

FIGURE 4 The wavelength-tuning response around (**a**) 1.249 μm, (**b**) 1.061 μm and (**c**) 0.915 μm, respectively

Another benefit of the decagonal quasiperiodic scheme is that RGB light can be generated in multiple direc-

tions, while only one direction was available in cases of one-dimensional superlattices. For decagonal quasiperiodic structure, the unique property is its equality against tenfold axis. The abovementioned generation of RGB light can be equally obtained when the crystal is rotated by integral multiples of $\pi/5$, which agrees well with the tenfold rotational symmetry of the two-dimensional decagonal superlattice.

3 Conclusions

In summary, we have demonstrated effective three primary colors coherent radiation of red at 624.5 nm, green at 530.5 nm and blue at 457.5 nm, by frequency doublings in a decagonal quasiperiodic superlattice. The conversion efficiencies were 31.8% for the red, 29.6% for the green and 11.3% for the blue. This scheme would be an attractive way to obtain an effective RGB coherent source.

ACKNOWLEDGEMENTS The authors acknowledge the National Natural Science Foundation of China for their financial support (Grant No. 10474135).

REFERENCES

1 P. Baldi, C.G. Treviño-Palacios, G.I. Stegeman, M.P. De Micheli, D.B. Ostrowsky, D. Delacourt, M. Papuchon, Electron. Lett. **31**, 1350 (1995)
2 S.S. Yap, W.O. Siew, T.Y. Tou, S.W. Ng, Appl. Opt. **41**, 1725 (2002)
3 Q. Ye, L. Shah, J. Eichenholz, D. Hammons, R. Peale, M. Richardson, A. Chin, B.H.T. Chai, Opt. Commun. **164**, 33 (1999)
4 J. Capmany, Appl. Phys. Lett. **78**, 144 (2001)
5 J.J. Romero, D. Jaque, J. García Solé, A.A. Kaminskii, Appl. Phys. Lett. **81**, 4106 (2002)
6 E. Canelar, G.A. Torchia, J.A. Sanz-García, P.L. Pernas, G. Lifante, F. Cussó, Appl. Phys. Lett. **83**, 2991 (2003)
7 J. Liao, J.L. He, H. Liu, F. Xu, H.T. Wang, S.N. Zhu, Y.Y. Zhu, N.B. Ming, Appl. Phys. B **78**, 265 (2004)
8 H.X. Li, Y.X. Fan, P. Xu, S.N. Zhu, P. Lu, Z.D. Gao, H.T. Wang, Y.Y. Zhu, N.B. Ming, J. Appl. Phys. **96**, 7756 (2004)
9 T.W. Ren, J.L. He, C. Zhang, S.N. Zhu, Y.Y. Zhu, Y. Hang, J. Phys.: Condens. Matter **16**, 3289 (2004)
10 Z.D. Gao, S.N. Zhu, A.H. Kung, Appl. Phys. Lett. **89**, 181101 (2006)
11 B.Y. Gu, Y. Zhang, B.Z. Dong, J. Appl. Phys. **87**, 7629 (2000)
12 H. Liu, S.N. Zhu, Y.Y. Zhu, N.B. Ming, X.C. Lin, W.J. Ling, A.Y. Yao, Z.Y. Xu, Appl. Phys. Lett. **81**, 3326 (2002)
13 Y.W. Lee, F.C. Fan, Y.C. Huang, B.Y. Gu, B.Z. Dong, M.H. Zhou, Opt. Lett. **27**, 2191 (2002)
14 R.T. Bratfalean, A.C. Peacock, N.G.R. Broderick, K. Gallo, R. Lewen, Opt. Lett. **30**, 424 (2005)
15 P. Ni, B. Ma, X. Wang, B. Cheng, D. Zhang, Appl. Phys. Lett. **82**, 4230 (2003)
16 M.A. Kaliteevski, S. Brand, R.A. Abram, T.F. Krauss, P. Millar, R.M. De La Rue, J. Phys.: Condens. Matter **13**, 10459 (2001)
17 T. Janssen, Phys. Rep. **168**, 55 (1998)
18 N.G.R. Broderick, G.W. Ross, H.L. Offerhaus, D.J. Richardson, D.C. Hanna, Phys. Rev. Lett. **84**, 4345 (2000)
19 K.R. Parameswaran, J.R. Kurz, R.V. Roussev, M.M. Fejer, Opt. Lett. **27**, 43 (2002)